

Pre-treatment prognostic value of DCE-MRI vascular, texture, shape and size parameters compared to traditional survival indicators obtained from locally advanced breast cancer patients

Dr Pickles Martin D (PhD), Dr Lowry Martin (DPhil), Dr Gibbs Peter (PhD)

Centre for Magnetic Resonance Investigations, Hull York Medical School at University of Hull, Hull Royal Infirmary, Anlaby Road, Hull, HU3 2JZ, United Kingdom

Short title: Prognostic value of pre-treatment DCE-MRI metrics

For correspondence

Dr Martin D Pickles, Centre for Magnetic Resonance Investigations, Hull York Medical School at University of Hull, Hull Royal Infirmary, Anlaby Road, Hull, HU3 2JZ, UK

Tel: 0044 (0)1482 674091, Fax: 0044 (0)1482 320137, e-mail: m.pickles@hull.ac.uk

Funding Acknowledgment

This study was supported by the Yorkshire Cancer Research Centre for Magnetic Resonance Investigations endowment

Abstract

Objectives

To determine if associations exist between pre-treatment dynamic contrast enhanced-MRI (DCE-MRI) based metrics (vascular kinetics, texture, shape, size) and survival intervals. Further, to compare the prognostic value of DCE-MRI parameters against traditional pre-treatment survival indicators.

Materials and Methods

A retrospective study was undertaken. Approval had previously been granted for the retrospective use of such data and the need for informed consent was waived. Prognostic value of pre-treatment DCE-MRI parameters and clinical data was assessed via Cox's proportional hazards models (CPHM). The variables retained by the final overall survival CPHM were utilised to stratify risk of death within 5 years.

Results

One hundred and twelve subjects were entered into the analysis. Regarding disease free survival negative oestrogen receptor status, T3 or higher clinical tumour stage, large ($>9.8\text{cm}^3$) MR tumour volume, higher 95th percentile ($>79\%$) percentage enhancement and reduced (>0.22) circularity represented the retained model variables. Similar results were noted for the overall survival with negative oestrogen receptor status, T3 or higher clinical tumour stage, and large ($>9.8\text{cm}^3$) MR tumour volume again all been retained by the model in addition to higher (>0.71) 25th percentile area under the enhancement curve.

Accuracy of risk stratification based on either traditional (59%) or DCE-MRI (65%) survival indicators performed to a similar level. However, combined traditional and MR risk stratification resulted in the highest accuracy (86%).

Conclusion

Multivariate survival analysis has revealed that model retained DCE-MRI variables provide independent prognostic information complementing traditional survival indicators and as such could help to appropriately stratify treatment.

Keywords

Breast cancer

Neoadjuvant

DCE-MRI

Prognosis

Survival

Introduction

Neoadjuvant chemotherapy (NAC) has become the standard treatment for patients diagnosed with locally advanced breast cancer (LABC) and some large operable breast tumours prior to surgery and adjuvant therapies [1]. The objective of NAC is not simply to downstage the primary tumour, hopefully facilitating breast conserving surgery (BCS) [2], but also to eradicate distant micro-metastases [2]. For those patients undergoing NAC whom achieve a pathological complete response (pCR) a survival advantage has been reported [2, 3]. However, the response to NAC can be quite variable with the majority of patients not achieving pCR [4].

Presently, patients undergo treatment stratification based on traditional prognostic indicators such as disease stage and lesion descriptors [5]. However, following this strategy not only is the initial response to NAC variable but also the longer term survival [3].

Researchers are currently trying to identify potential biomarkers to facilitate individualised treatments, and a number of investigators have identified dynamic contrast enhanced MRI (DCE-MRI) as a potential biomarker of longer term survival. DCE-MRI vascular kinetics reflect blood flow, vascular density and vessel permeability [6]. Literature reports have highlighted associations between DCE-MRI vascular kinetics obtained prior to and/or early (post 1st or 2nd NAC cycle) during NAC and survival intervals [7-19]. DCE-MRI data is processed by studying changes in the signal intensity against time to derive vascular parameters. However, the static source DCE-MRI images can also provide information related to both tumour texture and shape. Texture analysis results in the quantification of grey-level intensity and spatial variation thereby providing textural features that characterise the underlying

structure of the object under investigation. Textural features have been previously described [20] and have been linked not only with traditional breast cancer prognostic indicators but also the initial response to NAC treatment [21]. Likewise tumour shape has also been associated with prognostic indicators [22]. We hypothesise that given the association with prognostic indicators that both texture and shape will also be associated with longer term survival along with DCE-MRI vascular kinetics.

If suitable biomarkers could be identified that can predict survival outcome prior to NAC, then decisions regarding treatment stratification could be taken even before the initiation of NAC. Treatments with higher levels of side effects and/or increased post treatment surveillance could be justified in cases where patients were predicted to have shorter survival intervals.

The aims of this study were to determine if any associations exist between pre-treatment DCE-MRI based parameters (vascular kinetics, texture, shape) and survival intervals [disease free (DFS) and overall survival (OS)], additionally, to compare the prognostic value of DCE-MRI parameters against traditional survival indicators obtained prior to NAC.

Materials and Methods

Study population

Patients scheduled for NAC are routinely referred to this Institute for breast MR examinations prior to treatment to facilitate baseline assessment of their disease. During the study period the NAC regime typically consisted of 4, three-weekly cycles of combined intravenous epirubicin (90 mg/m²) and cyclophosphamide (600 mg/m²) followed by four cycles of Docetaxel (100mg/m²). After successful down-staging of their disease patients underwent mastectomy or BCS. This initial treatment was followed by individually tailored adjuvant therapies.

A survival study was undertaken of LABC patients and large operable breast cancers that had undergone neoadjuvant chemotherapy. Approval had previously been granted for the retrospective use of such data, as this activity did not involve any non-clinical research scans or the retrieval of non-clinical patient information, informed consent was not sought. Information held locally on a breast cancer database was used to retrospectively identify women who had undergone NAC between April 2006 and December 2009. To be included in the survival database patients must have undergone a pre-treatment breast MRI examination, received at least four cycles of NAC, proceeded to surgery and adjuvant radiotherapy.

Traditional pre-treatment survival indicators were obtained from the results of pre-treatment biopsies and clinical examinations via the hospital's electronic note system.

MRI technique

All MR imaging was undertaken on a 3.0T scanner (GE Healthcare, Milwaukee, USA) in combination with the manufacture's 8 channel phased array breast coil, prior

to the initiation of NAC. In each case a DCE-MRI dataset was acquired utilising a 3 dimensional sagittal T1W fat nulled VIBRANT (Volume Imaging for Breast Assessment) sequence with the following parameters: TR/TE/TI 4.1/1.6/5ms, flip angle 8° , FOV 22 x 22cm or 20 x 20cm, slice/gap 4mm/0mm interpolated to 2mm/0mm, matrix 220x160, bandwidth 41.7kHz, parallel imaging x2. Median temporal (min. max.) resolution was 33.1 (23.5, 44.7) seconds.

At the start of the 3rd dynamic phase a bolus injection of gadolinium contrast agent (0.05 mmol/kg body weight) was delivered by a Spectris Solaris power injector (Medrad, Warrendale, PA, USA) immediately followed by a 20ml saline flush, total injection time 10 seconds for all patients. Between the start of the study period and July 2008 gadodiamide (Gd-DTPA-BMA, Omniscan, GE Healthcare, Oslo, Norway) was utilised as the gadolinium containing contrast agent however from July 2008 until the end of the study period gadoterate (Gd-DOTA, Dotarem, Paris, France) was used. The r_1 relaxivity in plasma at 37°C for gadodiamide and gadoterate at 3.0T are reported to be $3.8\text{-}4.2\text{ L mmol}^{-1}\text{ s}^{-1}$ and $3.3\text{-}3.7\text{ L mmol}^{-1}\text{ s}^{-1}$ respectively [24].

All processing steps were undertaken by a researcher with ten years' experience of breast MR analysis. Regions of interest and vascular kinetics were processed via software developed in-house utilising IDL language (Exelis Visual Information Solutions Inc., Boulder, CO, USA) to facilitate model free empirical analysis of the enhancement characteristics of the lesions. The analysis procedure is briefly outlined. Individual phases of the DCE-MRI dataset were visually inspected for significant motion related misalignment, if noted the subject was excluded from the analysis. Early arterial phase images (~ post 1 minute contrast injection) were

interrogated to facilitate whole lesion segmentation. On each slice that demonstrated tumour a seed point was selected and an iterative semi-automated ROI was generated. If multiple tumour foci were noted on a slice then an ROI was generated for each focus. In this manner a 3-dimensional volume of interest was generated. For DCE-MRI analysis the signal intensity time course was assessed in a pixel-by-pixel manner across all dynamic phases. Linear interpolation was employed to determine vascular parameters. Histogram analysis of the whole lesion was undertaken to allow an assessment of tumour heterogeneity and resulted in first order statistics (mean, SD, skew, kurtosis, median and percentiles – 5th, 10th, 25th, 75th, 90th, 95th) for the following model free empirical parameters:

1. Elmax – The maximum enhancement index recorded during the experiment,

$$\text{where enhancement index} = S_t/S_0 - 1$$

S_t is the signal at a given time and

S_0 represents the baseline signal.

2. Tmax – Time to maximum, the time (seconds) to reach the maximum enhancement index from a manually defined start of the uptake curve
3. Rise time (RT) – Time (seconds) to reach the half maximum enhancement index point from the start of the uptake curve.
4. nMITR –Maximum intensity time ratio (MITR), normalised to the baseline signal.
5. PC₃₀ – Percentage of the maximum enhancement index recorded 30 seconds from the onset of the enhancement curve.
6. Initial slope – Average gradient of the uptake curve between the start of the enhancement curve and 30 seconds later.

7. Final slope – Average gradient over the last 120 seconds of the enhancement curve.
8. AUC_{60} – Area under the enhancement curve at 60 seconds from the onset of enhancement.

Texture and shape parameters were processed utilising MatLab (MathWorks, Natick, MA, USA). ROI data was imported from the DCE-MRI processing step. Texture analysis resulted in second order statistical features as outlined by Haralick et al. [20] (f1-f14) and Conners et al. [24] (f15 and f16) from the whole tumour ROI data for 1 minute post-contrast injection images. To avoid data sparseness images were decimated via histogram equalisation to 16 grey levels. Co-occurrence matrices with a pixel distance of 1 were calculated along 0° , 45° , 90° and 135° and subsequently averaged, see Ahmed et al. [21] for more details.

Given the through-plane spatial resolution it was felt that 3 dimensional shape analyses was inappropriate. Consequently, shape parameters, circularity [25], complexity [26] and convexity [26] were obtained from the individual ROI with the largest surface area.

Finally, MRI based size parameters, longest dimension (LD) and volume, were determined from the ROI data and entered into the survival analysis. MR based processing steps are illustrated in Figure 1.

Statistical Analysis

Subjects were followed up for five years following NAC treatment. To obtain survival data a final review of patients' electronic notes was undertaken in January 2015. Patients were categorised as having a critical survival event or censored. Critical events were defined as local tumour recurrence and/or metastasis (DFS) or a cancer related death (OS). Patients without critical events or lost to follow up, but known to be well at their most recent follow-up, were censored. The DFS and OS time interval was defined as the time from initiation of NAC to critical or censored event.

Both traditional prognostic indicators and DCE-MRI parameters underwent univariate Cox's proportional hazards model analysis. To facilitate survival analysis traditional prognostic indicators were dichotomised as follows: age (≤ 45 years or > 45 years), grade (I and II or III), histological type (special type or no special type), oestrogen receptor (ER) status (negative or positive), progesterone (PR) status (negative or positive), human epidermal growth factor receptor 2 (HER2) status (negative or positive), intrinsic subtype (triple negative or all other), T stage ($\leq T2$ or $> T2$), and N stage (N0 or $\geq N1$). To allow appropriate dichotomisation of DCE-MRI parameters the Youden's Index [27] was utilised to highlight a suitable threshold for each MR parameter.

To allow an assessment of interactions between individual parameters a multivariate Cox's proportional hazards model was employed. However, in an attempt to streamline the number of variables entered into the model, while allowing a comparison with all traditional prognostic indicators, only those MR parameters that demonstrated a significant ($p \leq 0.025$) univariate results were subsequently entered into the multivariate model. By lowering the alpha level the number of MR

parameters entered into the multivariate analysis was restricted in the hope of increasing model generalisation.

Following the multivariate overall survival analysis retained variables were used to stratify risk of death within 5 years of initiation of NAC treatment. For each subject the individual hazard ratios (HR) were summed for two separate groups, traditional prognostic indicators and MR parameters. While for a third combined group (traditional plus MR) previously calculated hazard ratio scores were summed. To facilitate appropriate dichotomisation of the hazard ratio score the Youden's Index [27] was utilised. Once dichotomised each group underwent Kaplan-Meier analysis.

All statistical analyses were undertaken utilising IBM SPSS version 20.0 (New York, USA) and MedCalc version 12.1, MedCalc Software (Ostend Belgium).

Results

Following a review of the local breast cancer database 138 potential subjects were identified. However 26 cases were excluded for a variety of reasons; incomplete MR data (4); less than 4 cycles of NAC (3); did not proceed to surgery (11); did not undergo radiotherapy (5); changed from curative to palliative intent (2); and incomplete clinical data held locally (1). Table 1 presents the pre-treatment lesion characteristics, clinical and treatment information for the 112 subjects that were entered into the survival analysis.

Regarding DFS, 29 critical events were noted and 83 subjects were censored. The median follow up interval for the whole DFS cohort was 60 months (min. 8, max. 60 months). When considering OS, 24 cancer related deaths were recorded and 88 patients were censored. The median follow up interval for the whole OS group was 60 months (min. 12, max. 60 months). Table 2 presents the follow up intervals for critical and censored subjects for both DFS and OS.

Univariate Cox proportional hazards model results for both traditional survival indicators and MRI parameters are presented in Table 3 and 4 respectively. Significant results for traditional survival indicators remained constant between the DFS and OS analysis with ER_(-ve), PR_(-ve), intrinsic subtype_(triple negative), T stage_(≥T3), and N stage_(≥N1) status all resulting in increased hazard. T stage status resulted in the highest hazard ratio for both disease free and overall survival. The T stage status for OS resulted in a considerably higher hazard ratio compared to the other significant results, whereas for the DFS analysis T stage hazard ratio was only marginally higher than the other traditional indicators.

The univariate results for MR parameters revealed significant results for size, vascular kinetic, texture and shape based metrics. Again consistent trends were noted between the disease free and overall survival results. Results for MR based tumour size indicators (longest dimension or volume) were associated with highly significant elevated hazard ratios. Whereas the maximum enhancement achieved (Elmax), rate of enhancement (RT, PC₃₀, and initial slope), and the amount of contrast agent delivered to and retained by the tumour over 60 seconds (AUC₆₀) revealed significant hazard ratio results for vascular kinetics for both disease free and overall survival. Additionally, significant results were also noted for nMITR and final gradient when considering DFS and Tmax for the OS analysis. Texture features [f7 (sum variance), f8 (sum entropy), f15 (cluster shade) and f16 (cluster prominence)] were consistently associated with survival for both disease free and overall survival. When considering shape parameters complexity was identified as a significant measure for both disease free and overall survival while circularity and convexity were only significant for the disease free analysis.

All traditional prognostic indicators along with significant ($p \leq 0.025$) univariate survival analysis DCE-MRI parameters were entered into multivariate models. To be entered into a model subjects had to have all necessary data. For six individuals at least one piece of information (e.g. histological grade) was unavailable consequently 106 subjects were entered into the multivariate models. The results of the Cox's proportional hazards models are presented in Tables 5 and 6 for DFS and OS respectively. When considering DFS negative ER receptor status (HR 2.08), T3 or higher clinical tumour stage (HR 2.34), large ($>9.8\text{cm}^3$) MR tumour volume (HR 4.93), higher 95th percentile ($>78.96\%$) PC₃₀ (HR 4.17) and reduced (>0.22)

circularity (HR 3.94) represented the retained model variables. Not only were the DCE-MRI based retained model variables associated with higher hazard ratios than the retained traditional survival indicators, but the level of significance attached to the hazard ratios was also at a much higher level. Similar results were noted for the overall survival multivariate analysis with negative ER receptor status (HR 5.38), T3 or higher clinical tumour stage (HR 4.30), and large ($>9.8\text{cm}^3$) MR tumour volume (HR 3.58) again all were retained by the model in addition to higher (>0.71) 25th percentile AUC_{60} (HR 5.73).

By utilising the retained variables from the overall survival analysis subjects were stratified into risk of death (high and low) within five years of initiation of NAC, for the 110 individuals where all data (ER receptor status, T-stage, MR tumour volume, and 25th percentile AUC_{60}) was available. Resulting Kaplan-Meier plots are illustrated in Figure 2 while Table 7 presents the results of the risk stratification compared to subject outcome (alive or dead). Kaplan-Meier logrank test results revealed highly significant differences in mean survival intervals for all three risk groups (traditional: low risk 58.7 months (56.9 – 60.5), high risk 49.4 months (45.2 – 53.6), $p=0.0005$; DCE-MRI: low risk 58.5 months (56.4 – 60.5), high risk 48.2 months (43.7 – 52.8), $p=0.0001$; and combined: low risk 57.5 months (55.6 – 59.3), high risk 33.9 months (25.8 – 42.0), $p<0.0001$). Risk stratification based on either traditional or DCE-MRI survival indicators performed to a similar level. However, combined traditional and MR risk stratification resulted in the most significant difference in survival intervals between the low and high risk groups.

Discussion

The vast majority of LABC patients who die from their disease do not die due to their primary tumour but from the consequences of metastatic spread [28]. Since elevated levels of neoangiogenesis enhance the likelihood of metastatic spread [29] there is an opportunity to identify individuals at higher risk of metastatic spread, and subsequently shorter survival intervals, via biomarkers that reflect tumour driven neoangiogenesis. The ability to identify patients at higher risk of shorter survival intervals could facilitate individualised treatments whereby more aggressive treatments and/or increased surveillance could be justified.

DCE-MRI has been proposed as such a biomarker since DCE-MRI vascular kinetics have been correlated with both micro-vessel density, perfusion and pro-angiogenic factors such as VEGF [6, 30]. Further, given the correlation with traditional prognostic indicators we hypothesise that both texture [21] and shape [22] obtained from DCE-MRI datasets will also be associated with survival intervals.

Previous studies have demonstrated the potential of MR based metrics as a pre-treatment imaging biomarker of longer term survival [8-12, 15, 16, 19]. Generally, shorter survival intervals are associated with larger enhancing tumours [8, 10, 11, 15, 16, 19], type III enhancement curve [11], reduced mean transit time [12], elevated rates of signal enhancement [7, 9, 10, 19], high washout rates [7], large AUC values [10], and tumour surrounding stroma with high signal enhancement ratio [15].

This study has demonstrated via univariate Cox proportional hazards analysis that the risk of a shorter survival interval, both disease free and overall, is elevated in individuals with tumours displaying the following DCE-MRI based pre-treatment characteristics: large size (LD or volume); rapid, leptokurtic, positively skewed, heterogeneous enhancement [maximum enhancement achieved (Elmax) and rate of enhancement (RT, PC₃₀, and initial slope)]; large amounts of contrast agent delivered and retained by the tumour over 60 seconds (AUC₆₀); elevated textural features (sum variance, sum entropy, cluster shade, cluster prominence) and complex lesion shape. Univariate analysis of traditional prognostic indicators available prior to NAC treatment revealed negative hormone receptor status (ER and PR), triple negative intrinsic subtype, large primary tumour ($\geq T3$) and positive nodal status ($\geq N1$) all to be associated with shorter survival intervals (DFS and OS).

Interactions between pre-treatment MR and traditional prognostic indicators were considered via multivariate survival analysis. Oestrogen receptor status, T stage and MR volume were all retained by both DFS and OS models with the addition of AUC₆₀ for OS and PC₃₀ and circularity for DFS. Although ER status and T stage were retained by the models a number of established traditional prognostic indicators such as nodal status, histological grade and HER2 status were not included in the final models. While higher, more significant hazard ratios were noted for MR parameters in the DFS model all retained variables were of a similar prognostic value for the OS analysis. For both disease free and overall survival models MR parameter provided independent prognostic information in addition to the traditional prognostic indicators.

When considering the vascular kinetics the pixel-by-pixel nature of the analysis allowed for an assessment of lesion heterogeneity. Interestingly, in keeping with current thinking [30-35] the mean and median values were of little prognostic value with only mean and median AUC_{60} values demonstrating any significant univariate results. This presumably reflected the fact that given the heterogeneous nature of breast tumours, mean and median metrics do not sufficiently characterise the tumour [32,35]. Literature reports have highlighted that quantification of tumour heterogeneity is associated with grade, treatment response and prognosis [30-35]. Typically, poorer prognosis is associated with high levels of entropy, kurtosis, standard deviation and positive skewness [32, 34]. This heterogeneous signature of poor prognosis was observed for both vascular and texture parameters with rapid, leptokurtic, positively skewed, heterogeneous vascular kinetics in addition to textural features indicating heterogeneous enhancement (sum variance, sum entropy, cluster shade, cluster prominence) all being associated with shorter survival intervals in this work.

The goal of identifying imaging biomarkers of longer term survival is to facilitate individualised treatments. By utilising the hazard ratios from the overall survival analysis, it was possible to stratify patients into low or high risk of death within 5 years of the initiation of NAC treatment, for traditional, MR and combined prognostic indicators. Stratification based on traditional prognostic indicators and MR parameters, in isolation, performed to a similar level with around 5% of cases identified as low risk dying within 5 years of NAC and therefore considered undertreated. Whereas for the high risk group around 65% of cases were still alive at the end of 5 years and therefore represented an over-treated population. Overall prediction accuracy was 59.1% and 64.5% for traditional and MR parameters

respectively. When traditional and MR prognostic indicators were combined the number of over-treated cases was dramatically reduced by over half to 30% at the expense of an increased undertreated population (10%). Nevertheless, the prediction accuracy was considerably higher at 86.4% than the traditional or MR risk stratification results. This result not only demonstrates the added prognostic value of pre-treatment DCE-MRI parameters to traditional survival indicators but also the potential usefulness of this approach for tailored therapies.

A number of limitations are highlighted when considering this study. Firstly, this study represents a single centre retrospective analysis of 112 subjects and as such the results might not reflect the wider population. Further, the ability to implement the findings of this report might be restricted given the utilised image protocol. In particular, variable temporal resolution, a change in FOV, a change in contrast agent and the utilised contrast dose might all affect the generalisation of this study's results. Secondly, while an attempt to avoid overparameterisation in the multivariate analysis was made the resulting models were close to the subjects per feature lower limit of 5 [35] (DFS 5 subjects/feature, OS 6 subjects/feature). Thirdly, given the retrospective nature of this study dichotomisation of MR parameters based on the Youden index may not be applicable to a wider population. Additionally, the results of the multivariate analysis were not validated on an independent cohort, consequently, the generalisation of the model is unknown. Finally, a number of papers [9, 12, 18, 19] have reported that early (post 1st or 2nd NAC cycle) changes from pre-treatment MR parameter values hold prognostic value. Unfortunately, due to local clinical practice this early NAC MR data was not available for this cohort.

In conclusion this study not only concurs with previous reports that DCE-MRI vascular kinetic and volume obtained prior to NAC treatment have prognostic value

but also finds that pre-treatment DCE-MRI based texture and shape metrics are also associated with survival intervals. Further, multivariate analysis revealed that model retained DCE-MRI variables provide independent prognostic information complementing traditional survival indicators. Finally, treatment stratification based on multivariate model retained variables resulted in higher prediction accuracy when traditional and DCE-MRI parameters were combined. While these results require validation from a much larger population it seems that DCE-MRI parameters acquired even before the initiation of NAC treatment are associated with survival intervals and as such can help to appropriately stratify treatment.

Acknowledgments

To follow after blind review process

References

1. Mamounas EP. Impact of Neoadjuvant Chemotherapy on Locoregional Surgical Treatment of Breast Cancer. *Ann. Surg. Oncol.* 2015;22:1425-1433.
2. Kuhl CK. The Changing World of Breast Cancer: A Radiologist's Perspective. *Invest. Radiol.* 2015;50:615-628.
3. van de Hage JH, van de Velde CCJH, Mieog SJS. Preoperative chemotherapy for women with operable breast cancer. *Cochrane Database of Systematic Reviews* 2007, Issue 2. Art. No.:CD005002. DOI: 10.1002/14651858.CD005002.pub2.
4. Houssami N, Macaskill P, von Minckwitz G, et al. Meta-analysis of the association of breast cancer subtype and pathological complete response to neoadjuvant chemotherapy. *European Journal of Cancer.* 2012;48:3342-3354.
5. Connolly RM, Stearns V. Current approaches for neoadjuvant chemotherapy in breast cancer. *Eur J Pharmacol.* 2013;717:58-66.
6. Padhani A and Khan AA. Diffusion-weighted (DW) and dynamic contrast-enhanced (DCE) magnetic resonance imaging (MRI) for monitoring anticancer therapy. *Targ. Oncol.* 2010;5:39-52.
7. Bone B, Szabo BK, Perbeck LG, et al. Can contrast-enhanced MR imaging predict survival in breast cancer? *Acta Radiol.* 2003;44:373-378.
8. Partridge SC, Gibbs JE, Essermann LJ, et al. MRI measurements of breast tumour volume predict response to neoadjuvant chemotherapy and recurrence-free survival. *Am J Roentgenol.* 2005;184:1774-1781.

9. Johansen R, Jensen LR, Rydland J, et al. Predicting survival and early clinical response to primary chemotherapy for patients with locally advanced breast cancer using DCE-MRI. *J Magn Reson Imaging*. 2009;29:1300-1307.
10. Pickles MD, Manton DJ, Lowry M, et al. Prognostic value of pre-treatment DCE-MRI parameters in predicting disease free and overall survival for breast cancer patients undergoing neoadjuvant chemotherapy. *Eur J Radiol*. 2009;71:498-505.
11. Heldahl MG, Bathen TF, Rydland J, et al. Prognostic value of pretreatment dynamic contrast-enhanced MR imaging in breast cancer patients receiving neoadjuvant chemotherapy: Overall survival prediction from combined time course and volume analysis. *Acta Radiol*. 2010;6:604-612.
12. Li SP, Makris A, Beresford MJ, et al. Use of dynamic contrast-enhanced MR imaging to predict survival in patients with primary breast cancer undergoing neoadjuvant chemotherapy. *Radiology*. 2011;260:68-78.
13. Tuncbilek N, Tokatli F, Altaner S, et al. Prognostic value DCE-MRI parameters in predicting factor disease free survival and overall survival for breast cancer patients. *Eur J Radiol*. 2012;81:863-867.
14. Dietzel M, Zoubi R, Vag T, et al. Association between survival in patients with primary invasive breast cancer and computer aided MRI. *J Magn Reson Imaging*. 2013;37:146-155.
15. Jones EF, Sinha SP, Newitt DC, et al. MRI enhancement in stromal tissue surrounding breast tumours: Association with recurrence free survival following neoadjuvant chemotherapy. *Plos One*. 2013;8:1-8.
16. Yi A, Cho N, Im S-A, et al. Survival outcomes of breast cancer patients who receive neoadjuvant chemotherapy: Associations with dynamic contrast-

enhanced MR imaging with computer-aided evaluation. *Radiology*. 2013;268:662-672.

17. Jafri NF, Newitt DC, Kornak J, et al. Optimized Breast MRI Functional Tumor Volume as a Biomarker of Recurrence-Free Survival Following Neoadjuvant Chemotherapy. *J. Magn. Reson. Imaging*. 2014;40:476-482.
18. Woolf DK, Padhani AR, Taylor NJ, et al. Assessing response in breast cancer with dynamic contrast-enhanced magnetic resonance imaging: Are signal intensity-time curves adequate? *Breast Cancer Res Treat*. 2014;147:335-343.
19. Pickles MD, Lowry M, Manton J, et al. Prognostic value of DCE-MRI in breast cancer patients undergoing neoadjuvant chemotherapy: a comparison with traditional survival indicators. *Eur. Radiol*. 2015;25:1097-1106.
20. Haralick RM, Shanmugam K, Dinstein I. Textural features for image classification. *IEEE Syst Man Cybernet Soc* 1973;3:610-621
21. Ahmed A, Gibbs P, Pickles M, et al. Texture Analysis in Assessment and Prediction of Chemotherapy Response in Breast Cancer. *J. Magn. Reson. Imaging*. 2013;38:89-101.
22. Jeh SK, Kim SH, Kim HS, et al. Correlation of Apparent Diffusion Coefficient Value and Dynamic Magnetic Resonance Imaging Findings With Prognostic Factors in Invasive Ductal Carcinoma. *J Magn Reson Imaging*. 2011;33:102-109.
23. Hao D, Ai T, Goerner F, et al. MRI Contrast Agents: Basic Chemistry and Safety. *J Magn Reson Imaging*. 2012;36:1060-1071.
24. Connors RW, Trivedi MM, Harlow CA. Segmentation of a high-resolution urban scene using texture operators. *Comp Vision Graphics Image Pro*. 1984; 25:273–310.

25. Haralick RM. Measurement for Circularity of Digital Figures. IEEE Syst Man Cybernet Soc 1974;SMC4:394-396.
26. Rosenfeld A and Kak AC. (1982). Geometric Property Measurement. In: *Digital Picture Processing*. 2nd ed. San Diego: Academic Press Inc. 240-270.
27. Youden WJ. Index for rating diagnostic tests. *Cancer*. 1950;3:32-35.
28. Weigelt B, Peterse JL, van Veer LJ. Breast Cancer Metastasis: Markers and Models. *Nat Rev Cancer*. 2005;5:591-602.
29. Chambers AF, Groom AC, MacDonald IC. Dissemination and growth of cancer cells in metastatic sites. *Nat. Rev. Cancer*. 2002;2:563-572.
30. Yang X and Knopp MV. Quantifying Tumor Vascular Heterogeneity with Dynamic Contrast-Enhanced Magnetic Resonance Imaging: A Review. *J Biomed. Biotechnol*. 2011;Article ID 732848, 12 pages.
31. Jackson A, O'Connor JPB, Parker GJM, et al. Imaging Tumor Vascular Heterogeneity and Angiogenesis using Dynamic Contrast-Enhanced Magnetic Resonance Imaging. *Clin. Cancer Res*. 2007;13:3449-3459.
32. Just N. Improving tumour heterogeneity MRI assessment with histograms. *Brit. J. Cancer*. 2014;111;2205-2213.
33. Asselin MC, O'Connor JPB, Boellaard R, et al. Quantifying heterogeneity in human tumours using MRI and PET. *Eur. J. Cancer*. 2012;48:447-455.
34. Davnall F, Yip CSP, Ljungqvist G, et al. Assessment of tumor heterogeneity: an emerging imaging tool for clinical practice? *Insights Imaging*. 2012;3:573-589.
35. Alic L, Niessen WJ, Veenland JF. Quantification of Heterogeneity as a Biomarker in Tumor Imaging: A Systematic review. *Plos One*. 2014;9:e110300.

Table 1 Pre-treatment lesion characteristics, clinical and treatment information

Parameter	Patients	Percentage
Histological grade		
Grade I	10	8.9
Grade II	45	40.2
Grade III	53	47.3
Missing	4	3.6
Histological type		
NST	34	30.4
Ductal	59	52.7
Lobular	16	14.3
Mucinous	1	0.9
Missing	2	1.8
Oestrogen receptor		
Negative	30	26.8
Positive	80	71.4
Missing	2	1.8
Progesterone receptor		
Negative	51	45.5
Positive	59	52.7
Missing	2	1.8
HER2		
Negative	94	83.9
Positive	18	16.1
Intrinsic type		
Luminal A	43	38.4
Luminal B/HER2 negative	19	17.0
Luminal B/HER2 positive	15	13.4
HER2 positive	3	2.7
Triple negative	27	24.1
missing	5	4.5
T stage		
≤T2	61	54.5
≥T3	51	45.5

Parameter	Patients	Percentage
N stage		
N0	73	65.2
≥N1	39	34.8
Age		
≤45	32	28.6
>45	80	71.4
NAC regime		
ECT	70	62.5
ECT _m	21	18.8
NTT1	8	7.1
NTT2	7	6.3
EC	2	1.8
NTT1 _m	1	0.9
EC _m	1	0.9
DC _m	1	0.9
C	1	0.9
Surgery post NAC		
Mastectomy	50	44.6
Breast conserving surgery	62	55.4
Adjuvant therapy		
Radiotherapy (Rx)	26	23.2
Rx with Hx and/or Cx	86	76.8

NAC regimes:

ECT epirubicin, cyclophosphamide and taxane

NTT1 (Neo-tAnGo trial protocol) epirubicin and cyclophosphamide with paclitaxel

NTT2 (Neo-tAnGo trial protocol) epirubicin and cyclophosphamide with paclitaxel + gemcitabine

EC Epirubicin and cyclophosphamide

DC Docetaxel and cyclophosphamide

C Capecitabine

Alteration (reduced number of cycles or dose) to intended NAC regime denoted by _m

Rx radiotherapy; Hx hormonal therapy; Cx chemotherapy

HER2 (human epidermal growth factor receptor 2)

Table 2 DFS and OS follow up intervals for critical and censored individuals

Event	n (%)	Median (min.-max.) months
DFS critical event	29 (26%)	20 (8 – 53)
DFS censored	83 (74%)	60 (19 – 60)
OS critical event	24 (21%)	26 (12 - 59)
OS censored	88 (79%)	60 (19 – 60)

Table 3 Significant traditional prognostic indicators univariate Cox proportional hazards model results

Variable	n	Disease free survival			Overall survival		
		Hazard ratio	95% CI	p value	Hazard ratio	95% CI	p value
ER							
+ve	80	1.000			1.000		
-ve	30	3.687	1.730 – 7.855	0.001	3.746	1.650 – 8.501	0.002
PR							
+ve	59	1.000			1.000		
-ve	51	2.751	1.235 – 6.128	0.013	3.168	1.302 – 3.168	0.011
Intrinsic type							
All other	80	1.000			1.000		
Triple negative	27	3.451	1.620 – 7.349	0.001	3.389	1.494 – 7.689	0.003
T stage							
≤T2	61	1.000			1.000		
≥T3	51	3.705	1.640 – 8.371	0.002	5.146	1.921 – 13.787	0.001
N stage							
N0	73	1.000			1.000		
≥N1	39	2.804	1.346 – 5.843	0.006	3.560	1.555 – 8.151	0.003

Table 4 Significant DCE-MRI based metric univariate Cox proportional hazards model results

Variable	n	Disease free survival			Variable	n	Overall survival		
		Hazard ratio	95% CI	p			Hazard	95% CI	p
Size				Size					
Longest dimension _(≤50mm)	67	1.000			Longest dimension _(≤50mm)	67	1.000		
Longest dimension _(>50mm)	45	4.859	2.149 – 10.988	<0.001	Longest dimension _(>50mm)	45	6.715	2.506 – 17.995	<0.001
Volume _(≤9.8cm³)	62	1.000			Volume _(≤9.8cm³)	62	1.000		
Volume _(>9.8cm³)	50	5.040	2.150 – 11.818	<0.001	Volume _(>9.8cm³)	50	7.688	2.623 – 22.530	<0.001
Vascular kinetics				Vascular kinetics					
					Tmax SD _(≤72.54sec)	30	1.000		
					Tmax SD _(>72.54sec)	82	4.335	1.019 – 18.438	0.047
					Elmax 5 th percentile _(≤1.16)	93	1.000		
					Elmax 5 th percentile _(>1.16)	19	2.602	1.113 – 6.082	0.027
					Elmax 10 th percentile _(≤1.30)	92	1.000		
					Elmax 10 th percentile _(>1.30)	20	2.413	1.032 – 5.638	0.042
					Elmax 25 th percentile _(≤1.49)	91	1.000		
					Elmax 25 th percentile _(>1.49)	21	2.351	1.006 – 5.495	0.048
Elmax 95 th percentile _(≤1.87)	60	1.000							
Elmax 95 th percentile _(>1.87)	52	2.166	1.023 -4.589	0.044					
Elmax SD _(≤0.48)	92	1.000							
Elmax SD _(>0.48)	20	3.102	1.079 – 8.918	0.032					
Elmax kurtosis _(≤0.74)	39	1.000							
Elmax kurtosis _(>0.74)	73	2.916	1.112 – 7.646	0.030					
					Rise time skew _(≤2.07)	34	1.000		
					Rise time skew _(>2.07)	78	3.370	1.005 – 11.302	0.049
Rise time kurtosis _(≤4.81)	25	1.000			Rise time kurtosis _(≤5.30)	28	1.000		
Rise time kurtosis _(>4.81)	87	4.502	1.070 – 18.936	0.040	Rise time kurtosis _(>5.30)	84	8.773	1.184 – 64.980	0.034

nMITR skew _(≤1.64)	45	1.000							
nMITR skew _(>1.64)	67	2.374	1.014 – 5.559	0.046					
PC ₃₀ 95 th percentile _(≤78.96%)	58	1.000			PC ₃₀ 95 th percentile _(≤78.96%)	58	1.000		
PC ₃₀ 95 th percentile _(>78.96%)	54	2.445	1.136 – 5.262	0.022	PC ₃₀ 95 th percentile _(>78.96%)	54	2.490	1.065 – 5.820	0.035
PC ₃₀ SD _(≤12.46%)	34	1.000							
PC ₃₀ SD _(>12.46%)	78	3.102	1.079 – 8.918	0.036					
PC ₃₀ skew _(>-0.12)	64	1.000							
PC ₃₀ skew _(≤-0.12)	48	2.112	1.008 – 4.424	0.048					
Initial upslope 75 th _(≤2.31)	84	1.000			Initial upslope 75 th _(≤2.31)	84	1.000		
Initial upslope 75 th _(>2.31)	28	2.194	1.035 -4.650	0.040	Initial upslope 75 th _(>2.31)	28	2.487	1.103 – 5.607	0.028
Initial upslope 90 th _(≤2.94)	88	1.000			Initial upslope 90 th _(≤2.94)	89	1.000		
Initial upslope 90 th _(>2.94)	24	2.239	1.040 – 4.819	0.039	Initial upslope 90 th _(>2.94)	23	2.646	1.157 – 6.053	0.021
					Initial upslope 95 th _(≤2.89)	79	1.000		
					Initial upslope 95 th _(>2.89)	33	2.340	1.048 – 5.227	0.038
Initial upslope SD _(≤0.37)	24	1.000							
Initial upslope SD _(>0.37)	88	4.236	1.007 – 17.819	0.049					
Final slope skew _(>-1.02)	69	1.000							
Final slope skew _(≤-1.02)	43	2.159	1.037 – 4.492	0.040					
Final slope kurtosis _(≤4.50)	69	1.000							
Final slope kurtosis _(>4.50)	43	2.159	1.037 – 4.492	0.040					
					AUC ₆₀ 25 th percentile _(≤0.71)	96	1.000		
					AUC ₆₀ 25 th percentile _(>0.71)	16	2.746	1.138 -6.627	0.025
AUC ₆₀ 90 th percentile _(≤1.23)	89	1.000			AUC ₆₀ 90 th percentile _(≤1.23)	90	1.000		
AUC ₆₀ 90 th percentile _(>1.23)	23	2.402	1.115 – 5.171	0.025	AUC ₆₀ 90 th percentile _(>1.23)	22	2.843	1.243 – 6.505	0.013
					AUC ₆₀ 95 th percentile _(≤1.37)	92	1.000		
					AUC ₆₀ 95 th percentile _(>1.37)	20	2.658	1.137 – 6.218	0.024
AUC ₆₀ mean _(≤0.77)	80	1.000			AUC ₆₀ mean _(≤0.77)	80	1.000		
AUC ₆₀ mean _(>0.77)	32	2.100	1.002 – 4.400	0.049	AUC ₆₀ mean _(>0.77)	32	2.472	1.106 – 5.522	0.027

					AUC ₆₀ median(≤ 0.77)	83	1.000		
					AUC ₆₀ median(> 0.77)	29	2.257	1.002 – 5.084	0.049
Texture					Texture				
f7, sum variance(≤ 73.21)	29	1.000			f7, sum variance(≤ 73.21)	29	1.000		
f7, sum variance(> 73.21)	83	3.614	1.093 – 11.948	0.035	f7, sum variance(> 73.21)	83	9.327	1.259 – 69.082	0.029
f8, sum entropy(≤ 4.93)	53	1.000			f8, sum entropy(≤ 4.93)	53	1.000		
f8, sum entropy(> 4.93)	59	4.173	1.698 – 10.260	0.002	f8, sum entropy(> 4.93)	59	7.533	2.244 – 25.284	0.001
f15, cluster shade(≤ -51.00)	74	1.000			f15, cluster shade(≤ -51.00)	74	1.000		
f15, cluster shade(> -51.00)	38	2.246	1.083 – 4.656	0.030	f15, cluster shade(> -51.00)	38	2.486	1.115 – 5.542	0.026
f16, cluster(≤ 10206.74)	29	1.000			f16, cluster(≤ 10295.75)	39	1.000		
f16, cluster(≤ 10206.74)	83	3.650	1.104 – 12.068	0.034	f16, cluster(> 10295.75)	73	4.381	1.306 – 14.695	0.017
Shape					Shape				
Complexity(≤ 28.19)	44	1.000			Complexity(≤ 28.19)	44	1.000		
Complexity(> 28.19)	68	4.806	1.671 – 13.819	0.004	Complexity(> 28.19)	68	3.709	1.267 – 10.858	0.017
Circularity(≤ 0.22)	45	1.000							
Circularity(> 0.22)	67	2.904	1.182 – 7.134	0.020					
Convexity(> 0.65)	76	1.000							
Convexity(≤ 0.65)	36	2.157	1.041 – 4.469	0.039					

Bold p value indicates MR variables entered into multivariate analysis

Table 5 Multivariate Cox's proportional hazards model results for DFS

Retained variable	Hazard ratio	Hazard ratio 95% CI	p value
ER _(-ve)	2.078	0.923 – 4.680	0.077
T stage _(≥T3)	2.339	0.887 – 6.169	0.086
MR volume _(>9.8cm³)	4.933	1.827 – 13.317	0.002
PC ₃₀ 95 th percentile _(>78.96%)	4.173	1.640 – 10.621	0.003
Circularity _(>0.22)	3.942	1.451 – 10.710	0.007

Table 6 Multivariate Cox's proportional hazards model results for OS

Retained variable	Hazard ratio	Hazard ratio 95% CI	p value
ER _(-ve)	5.382	2.029 – 14.279	0.001
T stage _(≥T3)	4.303	1.491 – 12.416	0.007
MR volume _(>9.8cm³)	3.578	1.142 – 11.210	0.029
AUC ₆₀ 25 th percentile _(>0.71)	5.730	1.995 – 16.458	0.001

Table 7 Risk of death within 5 years of NAC initiation compared to actual outcome

Variable type	Low risk			High risk			Overall accuracy
	Alive	Dead	Under treated	Alive	Dead	Over treated	
Traditional indicators	44	2	2/46 (4.3%)	43	21	43/64 (67.2%)	65/110 (59.1%)
MR based	51	3	3/54 (5.6%)	36	20	36/56 (64.3%)	71/110 (64.5%)
Combined traditional and MR	81	9	9/90 (10%)	6	14	6/20 (30%)	95/110 (86.4%)

Figure Legends

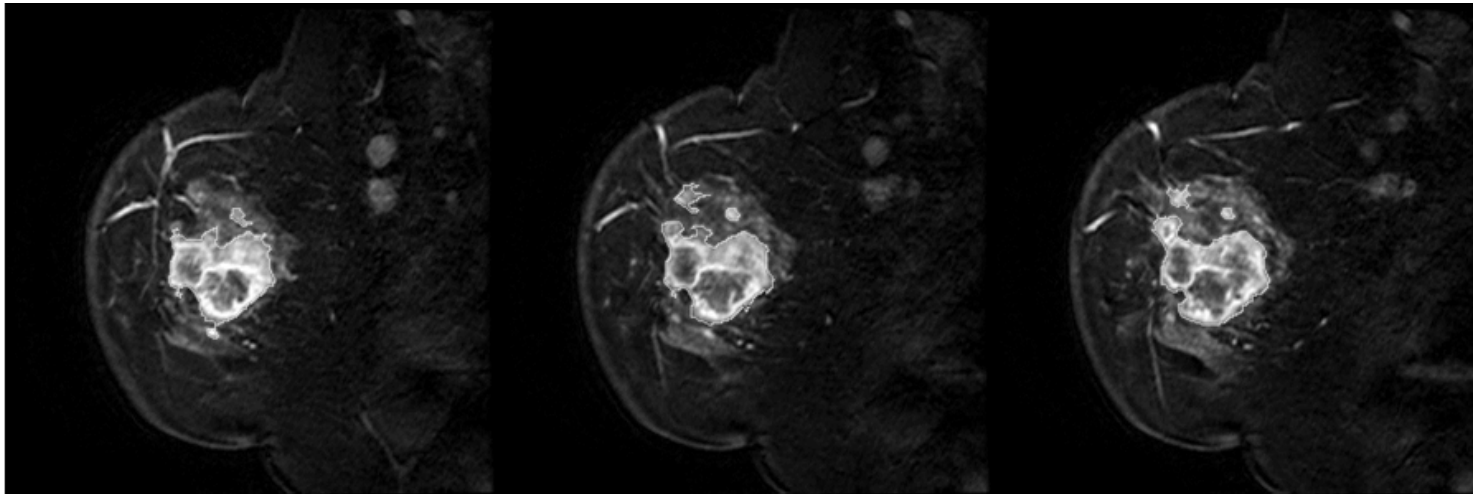
Figure 1

Schematic of MR data processing. Initially tumour segmentation was undertaken for each lesion containing slice. Following tumour segmentation vascular, texture and shape parameters were derived from the DCE-MRI data.

Figure 2

Resulting Kaplan-Meier plots from risk stratification based on overall survival analysis hazard ratios for (from left to right) traditional survival indicators, MR based prognostic factors and combined (traditional and MR) survival metrics. Combination of ER_(-ve) and T stage_(≤T2) results in a 0 score for traditional survival indicators while MR volume_(≤9.8cm³) and AUC₆₀ 25th percentile_(≤0.71) results in a 0 score for MR survival indicators.

Figure 1



Tumour segmentation on consecutive slices of primary and satellite foci. Resulting ROI data utilised to generate vascular, texture and shape parameters.

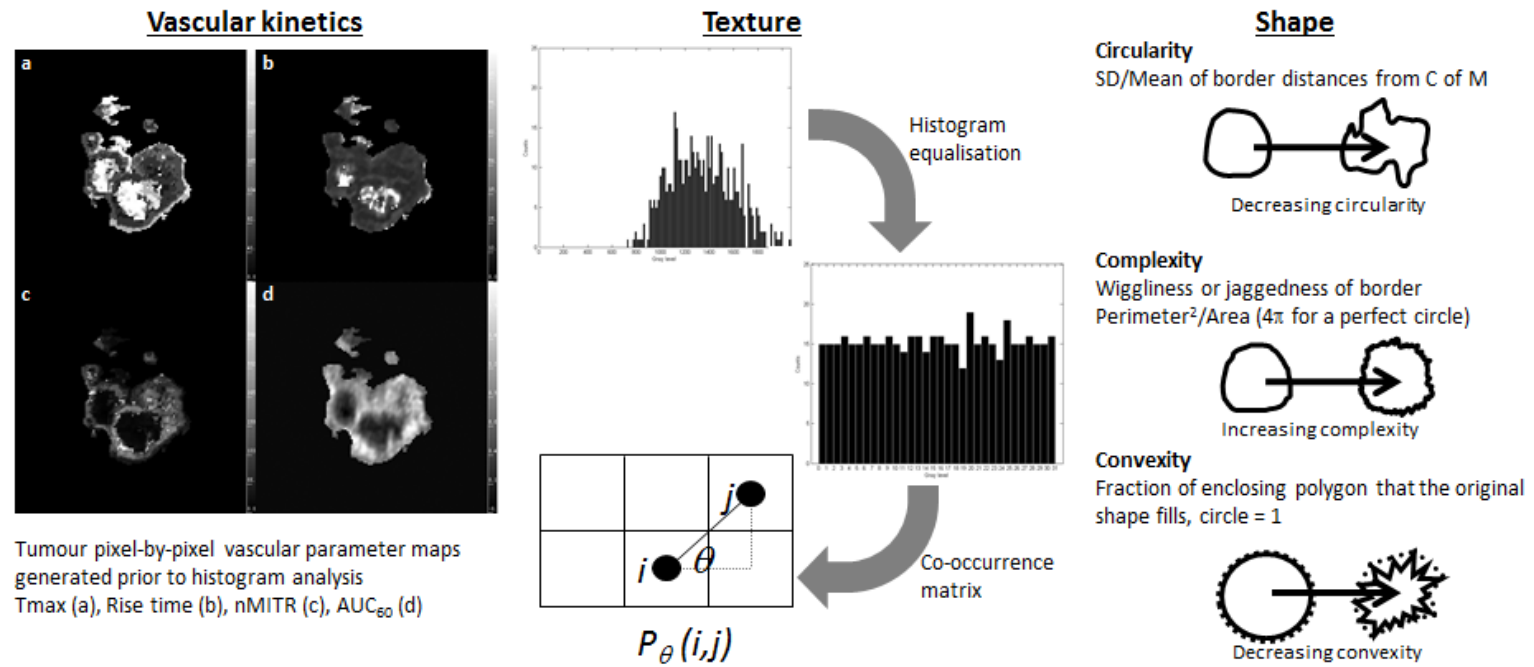


Figure 2

